JOURNAL OF AIRCRAFT
Vol. 31, No. 3, May–June 1994

Unique High-Alpha Roll Dynamics of a Sharp-Edged 65-Deg Delta Wing

L. E. Ericsson*
Lockheed Missiles & Space Company, Inc., Sunnyvale, California 94086
and
E. S. Hanff†
Institute for Aerospace Research, Ottawa, Ontario, Canada

An analysis has been performed of experimental results obtained in roll oscillation tests at 30-deg angle of attack of a 65-deg sharp-edged delta wing in order to uncover the fluid mechanical phenomena causing the unusual, highly nonlinear vehicle dynamics. In addition to the expected effect of convective flow time lag, the test results show highly nonlinear effects of the angular rate, which themselves are influenced by the effect of convective time lag. A flow hypothesis is presented that can explain the unusual experimental results.

Nomenclature

b = wing span
c = wing root chord
f = oscillation frequency
k = reduced frequency, $\omega b/2U_\infty$
l = rolling moment, coefficient $C_l = l/(\rho_\infty U_\infty^2/2)Sb$
M = Mach number
p = roll rate
Re = Reynolds number, $U_\infty c/\nu_\infty$
S = reference area, projected wing area
s = local semispan
t = time
U_∞ = freestream velocity
$\bar{U}$ = convection velocity
y = spanwise body-fixed coordinate, Fig. 10
z = vertical body-fixed coordinate, Fig. 10
α = angle of attack
β = angle of sideslip
Δ = increment or amplitude
Δt = time lag
$\Delta\phi$ = roll oscillation amplitude
θ_{LE} = leading-edge half-angle
Λ = leading-edge sweep angle, $\pi/2 - \theta_{LE}$
ν = kinematic viscosity
ξ = dimensionless x coordinate, x/c
ρ = air density
σ = inclination of body axis relative to freestream velocity
ϕ = roll angle
ϕ_0 = mean roll angle
$\bar{\phi}$ = reduced roll rate, $b\dot{\phi}/2U_\infty$
ω = angular frequency, $2\pi f$

Subscripts
LE = leading edge
max = maximum
V = vortex
∞ = freestream conditions

Differential Symbols
$\dot{\phi}$ = $\partial\phi/\partial t$: $C_{l\beta} = \partial C_l/\partial\beta$; $C_{l\phi} = \partial C_l/\partial\phi$
C_{lp} = $\partial C_l/\partial(bp/2U_\infty)$: $C_{l\dot{\beta}} = \partial C_l/\partial(b\dot{\beta}/2U_\infty)$
$C_{l\dot{\phi}}$ = $\partial C_l/\partial(b\dot{\phi}/2U_\infty)$

Introduction

RESULTS obtained in high-rate, large-amplitude roll oscillation tests at $M = 0.3$ and $Re = 2.4 \times 10^6$ of a sharp-edged 65-deg delta wing (Fig. 1) at 30-deg inclination of the roll axis relative to the freestream,[1,2] are unique in that they cannot be obtained by time-lagging static experimental results.[3] This is contrary to past experience, showing that the dynamic effects of separated flow on bodies of revolution[4] and slender wings[5] could be predicted simply by phasing the force or moment vector measured in static tests to account for the effect of convective flow time lag. The present tests show that there is a change of the magnitude of the rolling moment vector from its static value. A flow hypothesis is presented that can explain the unusual experimental results. No attempt is made here to formulate an aerodynamic prediction method.

Analysis

The static rolling moment exhibits highly nonlinear characteristics, caused by the breakdown of the leading-edge vortices (Fig. 2). (The solid line is an idealized representation of the experimental results, used later to construct Fig. 5b.) Breakdown occurs at the trailing edge of the delta wing at a certain angle of attack, and progresses forward as the angle of attack is increased further[6] (Fig. 3). Accounting for the bevel angle of the present model (Fig. 1), the angle of attack should be decreased by 5 deg.[7] That is, the 30-deg roll-axis attitude is represented by $\alpha = 25$ deg in the results for the flat-top model[6] in Fig. 3.

At a roll angle, the effective angle of attack and leading-edge sweep of the delta wing are given by

$$\alpha(\phi) = \tan^{-1}(\tan\sigma\cos\phi) \tag{1}$$

$$\Lambda(\phi) = \Lambda \pm \tan^{-1}(\tan\sigma\sin\phi) \tag{2}$$

The effective sweep of the wing half that rolls up (leeside wing half) increases, and that of the other decreases, resulting in an aft and forward shift, respectively, of the corresponding

Presented as Paper 92-0673 at the AIAA 30th Aerospace Sciences Meeting and Exhibit, Reno, NV, Jan. 6–9, 1992; received April 30, 1992; revision received Feb. 5, 1993; accepted for publication March 12, 1993.

*Retired; currently Engineering Consultant. Fellow AIAA.
†Senior Research Officer. Member AIAA.

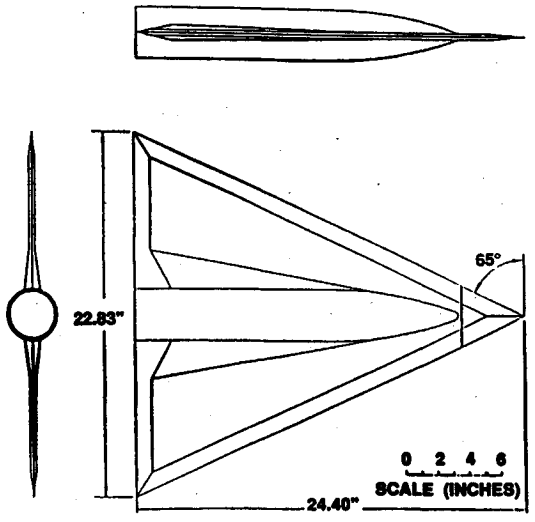

Fig. 1 Delta wing composite model.[1]

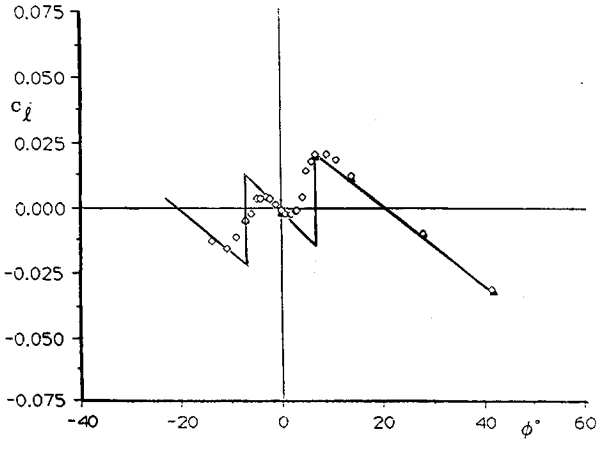

Fig. 2 Static $C_l(\phi)$ characteristics at σ = 30 deg of 65-deg delta wing.[2]

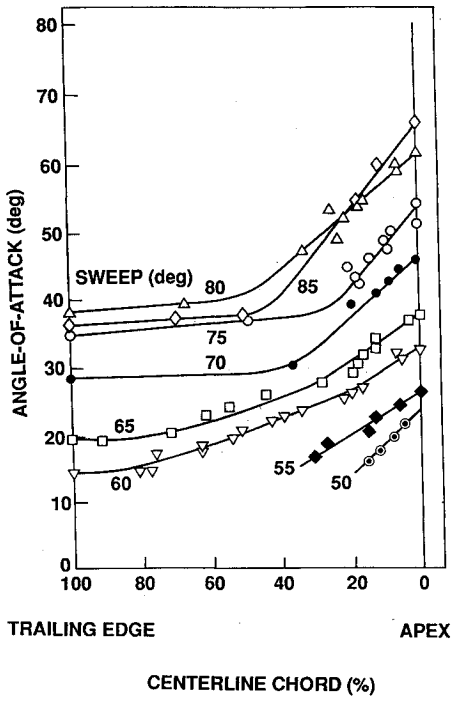

Fig. 3 Effect of angle of attack on vortex breakdown position on sharp-edged delta wings.[6]

vortex breakdown locations. It can be seen in Fig. 3 that small changes in effective sweep, i.e., <2 deg, corresponding to $|\phi| \approx 3$ deg at $\sigma = 25$ deg according to Eq. (2), result in rather small shifts in the position of the breakdown points (<10%). However, when the roll angle is increased beyond a certain value, the position of the breakdown point on the leeside wing half moves aft very rapidly, in fact creating a discontinuity as it suddenly jumps all the way past the trailing edge. Figure 3 shows that for $\alpha = 25$ deg this occurs at $\Lambda \approx 70$ deg, which according to Eq. (2) requires a roll angle $\phi \approx 9$ deg. This large shift of the breakdown point due to small roll angle variations leads to significant changes in the vortex-induced lift. This becomes the dominant mechanism, resulting in the static roll instability observed experimentally. It should be noted that the change in angle of attack, Eq. (1), under the above conditions, is insignificant (<0.4 deg).

For $|\phi| > 9$ deg, the fully attached vortex on the leeside wing half has a stabilizing effect, whereas the statically destabilizing effect of the vortex breakdown on the windward wing half becomes more and more insignificant because of the slow forward progression of the breakdown location (Fig. 3). This leads to the off-zero trim at $\phi \approx \pm 20$ deg. Thus, the static characteristics depicted in Fig. 2 can be explained in a straightforward manner.

Vehicle Dynamics

For slow oscillations, $k^2 << 1$, for which the phase lag $\omega\Delta t$ is small, one obtains the following vortex-induced contribution[8]:

$$\Delta C_l(t) = \Delta C_{l_\phi}\phi(t - \Delta t) \approx \Delta C_{l_\phi}[\phi(t) - \Delta t\dot{\phi}(t) + \ldots] \quad (3)$$

That is

$$\Delta C_{l_{\dot\phi}} = \partial\Delta C_l/\partial(b\dot\phi/2U_\infty) = -\Delta C_{l_\phi}(2xU_\infty/b\tilde{U}_V) \quad (4)$$

Equation (4) demonstrates how the time lag causes the dynamic effect to be opposite to the static effect. Thus, the statically destabilizing effect of vortex breakdown, discussed earlier, will be dynamically stabilizing,[8] as illustrated by the results for a 75-deg delta wing[9] shown in Fig. 4. The tick mark ending the predicted data trend[8] is where vortex breakdown is predicted to first occur on the delta wing, according to the results[6] in Fig. 3. Figure 4 shows the experimental results[9] to

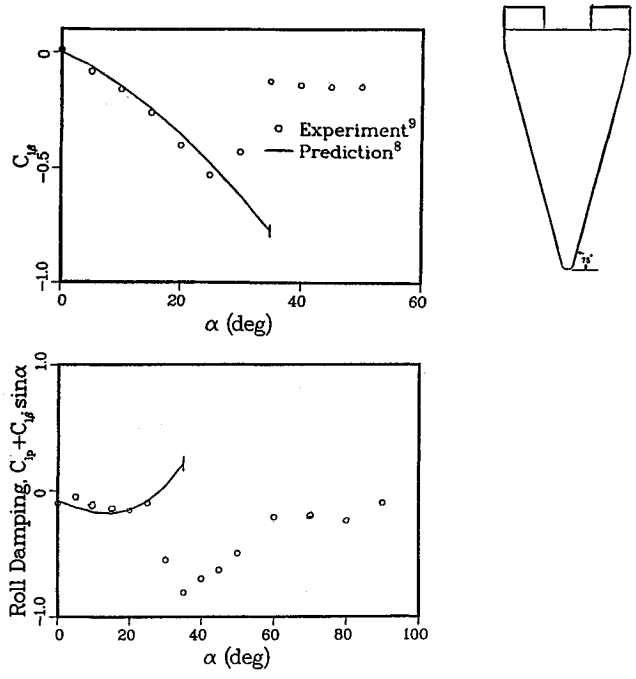

Fig. 4 Roll stability characteristics of flat 75-deg delta wing.

deviate from prediction[8] earlier than expected. This is the likely effect of support interference.[10] More important is the demonstrated effect of vortex breakdown, statically destabilizing, but dynamically stabilizing.

For the vortex-induced effects in Fig. 4, Eq. (4) applies with $\Delta C_{l_{\dot\phi}}$ substituted by $\Delta C_{l_{\dot\beta}}$ and ΔC_{l_ϕ} by ΔC_{l_β}. Assuming that the convective time lag from apex in the presence of vortex breakdown is the same as that for intact vortices[5] for which the convection velocity has been measured to be $\bar{U}_V = U_\infty/0.75$, one can apply Eq. (4) in the following manner. The effect of incipient vortex breakdown, located in an infinitesimally small region near the trailing edge, $x = c$ in Eq. (4), could for negligible influence of the downstream flow region be described by

$$\Delta C_{l_{\dot\beta}} = -0.75\Delta C_{l_\beta} \tan \Lambda \qquad (5)$$

Figure 3 shows vortex breakdown to move more or less discontinuously from the trailing edge to a location forward of midchord on slender delta wings, $\Lambda \geq 70$ deg. With this in mind, one may be justified to use Eq. (5) to describe the stepwise deviation from the predicted aerodynamic characteristics[8] in Fig. 4, as caused by vortex breakdown at $\alpha = 35$ deg.

The tick marks in Fig. 4 at $\alpha = 35$ deg indicate the roll stability values expected in the absence of vortex breakdown. Because C_{l_p} is small ($-0.1 < C_{l_p} < 0$), the difference between predicted and measured stability values at $\alpha = 35$ deg represents the maximum effect of vortex breakdown on the vortex-induced loads. Thus, $\Delta C_{l_\beta} \approx 0.65$ is obtained from Fig. 4, which for $\Lambda = 75$ deg in Eq. (5) gives $\Delta C_{l_{\dot\beta}} \approx -1.82$, or $\Delta C_{l_{\dot\beta}} \sin \alpha \approx -1.05$ for $\alpha = 35$ deg. This is in excellent agreement with $\Delta C_{l_{\dot\beta}} \sin \alpha \approx -1.0$, obtained from Fig. 4.

Combining this result with the fact that using the same time-lag concept provided good prediction[11,12] of the measured[13,14] limit cycle amplitude of the wing-rock oscillation of 80-deg delta wings, one would expect that the roll-stability characteristics of the present 65-deg delta wing could be described in a similar manner. The idealized static roll characteristics associated with wing rock are as sketched in Fig. 5a, according to the most recent analysis.[15] Applying the time-lag effect to the idealized static characteristics in Fig. 2 one obtains the characteristics sketched in Fig. 5b. The ones for the 80-deg delta wing have been documented.[11,15] In what follows it will be shown that the experimental roll characteristics of the 65-deg delta wing deviate dramatically from those in Fig. 5b, and the fluid mechanical reasons for this will be described.

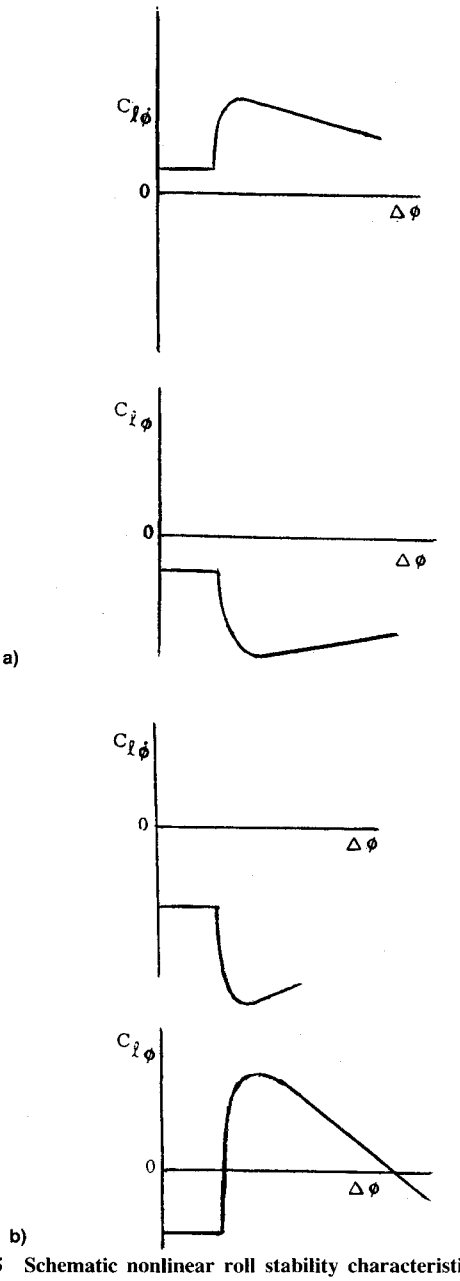

Fig. 5 Schematic nonlinear roll stability characteristics of 80- and 65-deg delta wings: a) $\Lambda = 80$ deg and b) $\Lambda = 65$ deg.

Discussion

The experimental results for the 65-deg delta wing[1] (Fig. 6) show that the roll damping derivative $C_{l_{\dot\phi}} = \partial C_l/\partial\dot\phi$, where $\dot\phi = \pm k\Delta\phi$ for the results at $\phi = 0$ in Fig. 6, does not change in any highly nonlinear fashion with the amplitude $\Delta\phi$, according to the $C_l(\dot\phi)$ slopes, contrary to the expectations based upon Fig. 5b. However, the effect of the reduced frequency on $C_{l_{\dot\phi}}$ is nonlinear (Fig. 7). The instantaneous values of C_l at the end points of the oscillation cycle, where $\dot\phi = 0$ and $\phi = \pm\Delta\phi$, are shown in Fig. 8. These $C_l(\phi)$ characteristics are also void of any highly nonlinear trend.

The measured dynamic characteristics, shown in Figs. 6–8, indicate that applying the time-lag effect to the separation-induced static characteristics, as in Eq. (4), is not sufficient for prediction of the measured dynamic characteristics. This implies that in addition to introducing a phase lag of the static rolling moment, the roll dynamics also change the magnitude of the vortex-induced rolling moment. A well known example of a similar motion-induced effect is the large dynamic-stall overshoot of static lift maximum.[16] In that case the pitching motion changes the effective geometry through pitch-rate-induced accelerated flow and moving-wall effects, providing a large overshoot of static lift maximum. A large part of this dynamic lift increase is a quasisteady-type effect.[16] That is, there exists, at least in theory, a geometrical shape change that would give the same lift increase in a static test. A similar roll-rate-induced effect on the lift and associated rolling moment seems to be present for the 65-deg sharp-edged delta wing.

Dynamic Camber Effect

The effect of static longitudinal camber on the vortex-induced loads measured on a 70-deg sharp-edged delta wing has been shown to be significant.[17] Even larger is the observed effect of longitudinal camber on the breakdown of the leading-edge vortex[18] (Fig. 9). For the same maximum local angle of attack α_{max} on the delta wing, a positive camber of $\Delta\alpha/\alpha_{max} = 1$ delays vortex breakdown to occur downstream of the trailing edge (Fig. 9a), whereas a negative camber of the same magnitude, $\Delta\alpha/\alpha_{max} = -1$, causes burst to occur very close to the apex (Fig. 9b). Obviously, for a pitching delta wing, the pitch-rate-induced camber will have similarly large effects on the breakdown of leading-edge vortices.

It is shown in Ref. 19 that the nonlinear lift characteristics of delta wings are determined by the ratio between the angle of attack and the leading-edge slope, the parameter being

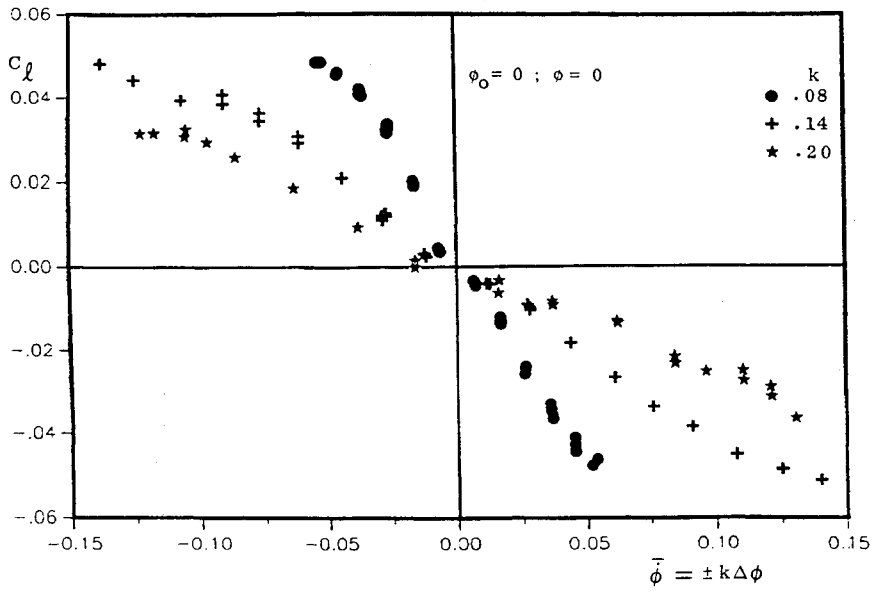

Fig. 6 $C_l(\bar{\phi})$ **characteristics of 65-deg delta wing at** $\sigma = 30$ **deg,** $\phi_0 = 0$, **and** $\phi = 0$.

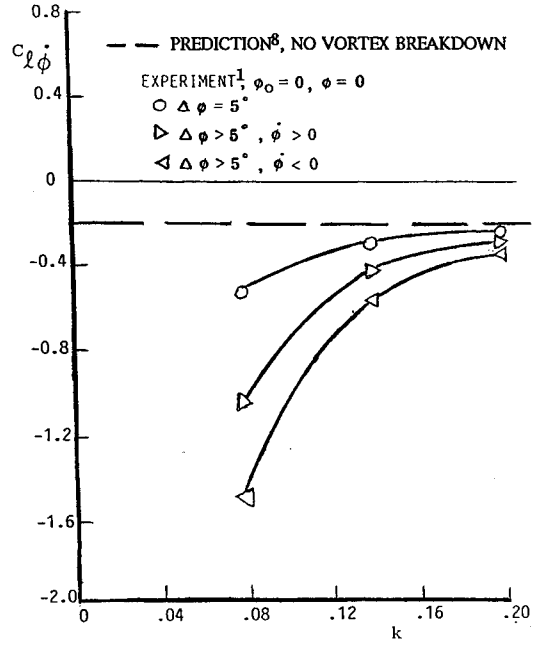

Fig. 7 Roll damping $C_{l\dot{\phi}}$ **as a function of** k **at** $\phi_0 = 0$ **and** $\phi = 0$.

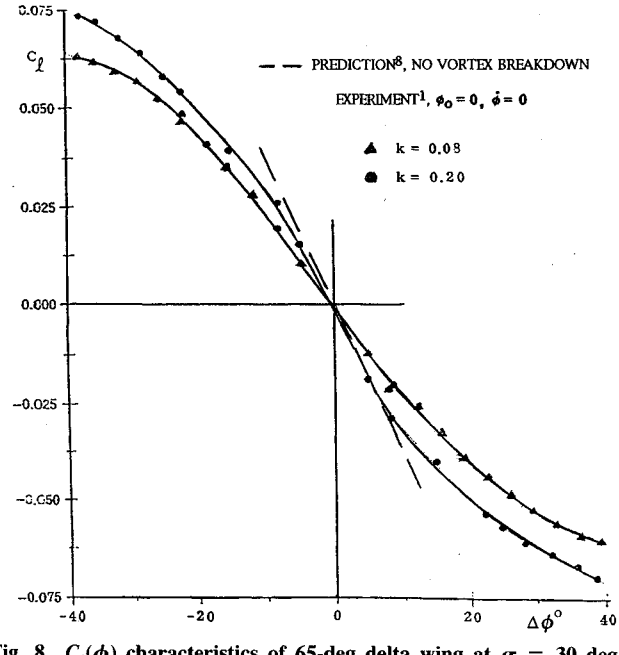

Fig. 8 $C_l(\phi)$ **characteristics of 65-deg delta wing at** $\sigma = 30$ **deg,** $\phi_0 = 0$, $\dot{\phi} = 0$.

$\tan\alpha/\tan\theta_{LE} \approx \alpha/\theta_{LE}$, where $\theta_{LE} = \pi/2 - \Lambda$. The roll-stability derivative $C_{l\beta}$ is also determined by this parameter.[19] Based upon the experimental results[20] in Fig. 10, it was suggested in Ref. 21 that the local α/θ_{LE} variation from apex to trailing edge would be very important, and that as a consequence, the roll-rate-induced camber effect would be very similar to the pitch-rate-induced camber effect. In both cases it is the motion-induced change of the local angle of attack at the leading edge that matters.

The local, roll-rate-induced camber is

$$\Delta\alpha_{LE} = \bar{\phi}\xi \sec\alpha \tag{6}$$

Thus, the total roll-rate-induced camber is

$$\Delta\alpha = (\Delta\alpha_{LE})_{\xi=1} = \bar{\phi} \sec\alpha \tag{7}$$

Where

$$|\bar{\phi}| = k\Delta\phi \tag{8}$$

At $\phi = \phi_0 = 0$ and $\alpha = \sigma = 30$ deg, Eqs. (7) and (8) give

$$|\Delta\alpha| \leq 2k\Delta\phi/\sqrt{3} \tag{9}$$

Thus, $|\Delta\alpha| \leq 9.2$ deg for $k \leq 0.2$ and $\Delta\phi \leq 40$ deg. This gives the ratio $|\Delta\alpha|/\alpha \leq 0.31$ for $\alpha = 30$ deg. This ratio is comparable in magnitude to the ratio $|\Delta\alpha|/\alpha = 1$, which produced the huge effects on vortex breakdown shown in Fig. 9.

According to Fig. 3, with $\alpha = 25$ deg representing $\alpha = 30$ deg, one would expect vortex breakdown to occur at 40% of the centerline chord downstream of apex if there were no roll-rate-induced camber effects at $\phi = 0$. When adding these effects one expects the induced conical camber for the "down-stroking" wing half, i.e., the starboard one for $\dot{\phi} > 0$ and the port one for $\dot{\phi} < 0$, to move vortex breakdown aft of 40% chord. On the opposite wing half the induced conical camber will move the breakdown forward of 40% chord. The roll-rate-induced camber, which is maximum at $\phi = 0$ for $\phi_0 = 0$, would provide a damping contribution that varies lin-

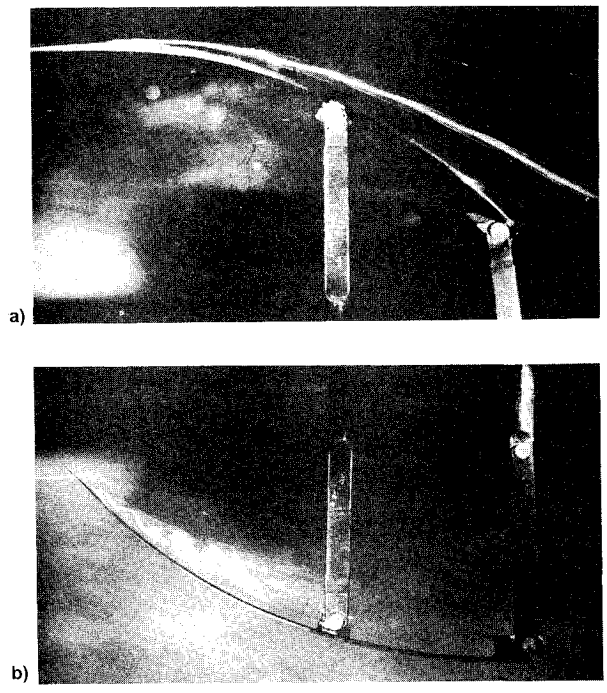

Fig. 9 Effect of longitudinal camber on the breakdown of the leading-edge vortex on an 80-deg delta wing[18]: local incidence a) increasing and b) decreasing with distance from apex.

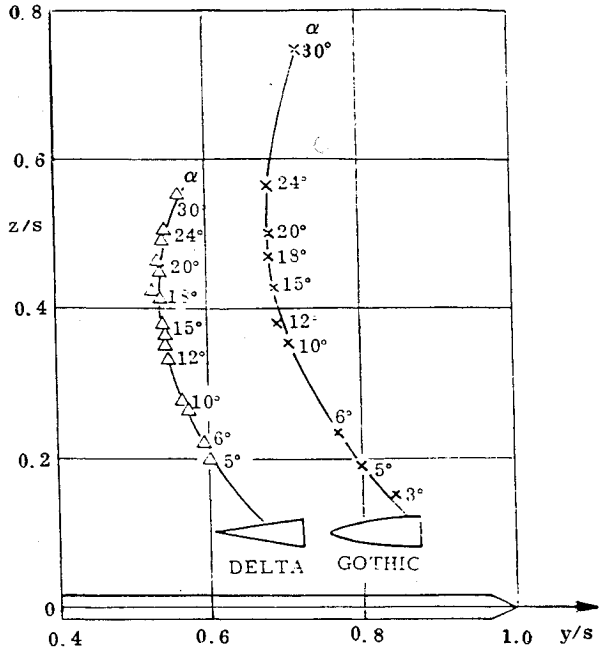

Fig. 10 Vortex position above the trailing edge of slender sharp-edged wings.[20]

early with the roll rate as long as the vortex breakdown characteristics are linear, i.e., for $\xi \leq 0.5$ in Fig. 3.

Figure 6 shows that the measured roll damping varies linearly with the amplitude $\Delta\phi$ for constant k. From the experimental results for $|C_l| \leq 0.04$, one obtains the $C_{l_{\dot{\phi}}}(k)$ characteristics shown in Fig. 7. The figure illustrates how increasing k diminishes the damping effect of vortex breakdown. Comparing the results in Fig. 5b with those in Figs. 6 and 7 one finds that in both cases the roll-damping characteristics are highly nonlinear. They are, however, very different in character. Instead of the expected nonlinear amplitude effect (Fig. 5b), the 65-deg delta wing exhibits linear $C_{l_{\dot{\phi}}}(\Delta\phi)$ characteristics (Fig. 6) together with very nonlinear effects of k (Fig. 7).

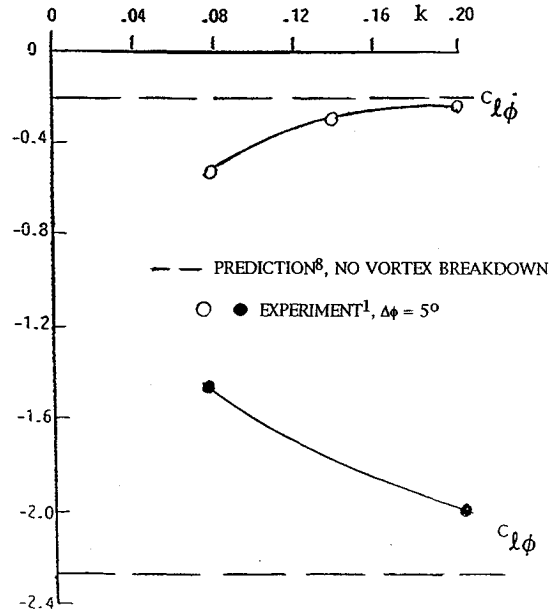

Fig. 11 Variation with k of the effect of vortex breakdown on dynamic and static stability derivatives.

The $C_l(\phi)$ characteristics for $\phi = 0$ in Fig. 8 are obtained for $\phi = \pm\Delta\phi$, at the end of the roll deflection, when $\dot{\phi} = 0$. Apparently, there exists a remnant roll-rate-induced camber effect at $\phi(t) = 0$, generated earlier when $|\phi(t - \Delta t)| \neq 0$. According to the results in Fig. 8, the remnant roll rate induces a conical camber at $\phi = \pm\Delta\phi$ that delays the aft movement of vortex breakdown on the leeside wing half. In addition, the induced positive camber delays the forward movement of vortex breakdown on the windward side. Therefore, the roll-rate induced remnant camber effect will generate statically stabilizing contributions on both wing halves, which increase with increasing k in agreement with the experimental data trend in Fig. 8. Figure 11 shows how the dynamic and static stability derivatives, defined by the experimental results for $\Delta\phi = 5$ deg in Figs. 6 and 8, respectively, vary with k. As expected, the statically destabilizing/dynamically stabilizing effect of vortex breakdown diminishes with increasing k.

Conclusions

An analysis of the highly nonlinear roll dynamics observed in high-rate, large-amplitude roll oscillation tests of sharp-edged, 65-deg delta wing, at a roll-axis inclination of 30 deg relative to the freestream, has led to the following conclusions.

1) Static and dynamic roll characteristics are largely determined by the effect of vortex breakdown.

2) The dynamic effect of vortex breakdown is to a large extent controlled by the roll-rate-induced conical camber.

3) The roll response to both roll angle and roll rate are subject to significant convective time-lag effects.

Acknowledgments

The authors are indebted to S. B. Jenkins and X. Z. Huang, Institute for Aerospace Research, Ottawa, for their valuable assistance in the presentation and evaluation of the experimental results, as well as to Jerry E. Jenkins, Wright Laboratories, Wright Patterson AFB, for his helpful comments.

References

[1]Hanff, E. S., and Jenkins, S. B., "Large-Amplitude High-Rate Roll Experiments on a Delta and Double Delta Wing," AIAA Paper 90-0224, Jan. 1990.

[2]Hanff, E. S., and Ericsson, L. E., "Multiple Roll Attractors of a Delta Wing at High Incidence," AGARD-CP-494, AGARD FDP Symposium on Vortex Flow Aerodynamics, Paper 31, Scheveningen, The Netherlands, Oct. 1990.

[3]Ericsson, L. E., "Analysis of Wind-Tunnel Data Obtained in High-Rate Rolling Experiments with Slender Delta Wings," National Research Council IAR-CR-14, Aug. 1991.

[4]Ericsson, L. E., and Reding, J. P., "Fluid Dynamics of Unsteady Separated Flow, Part I, Bodies of Revolution," *Prog. Aerospace Sci.*, Vol. 23, 1986, pp. 1–84.

[5]Ericsson, L. E., and Reding, J. P., "Fluid Dynamics of Unsteady Separated Flow, Part II, Lifting Surfaces," *Prog. Aerospace Sci.*, Vol. 24, 1987, pp. 249–356.

[6]Wendtz, W. H., and Kohlman, D. L., "Vortex Breakdown on Slender Sharp-Edged Delta Wings," AIAA Paper 69-778, July 1969.

[7]Ericsson, L. E., and King, H. H. C., "Effect of Leading-Edge Cross-Sectional Geometry on Slender Wing Unsteady Aerodynamics," AIAA Paper 92-0173, Jan. 1992.

[8]Ericsson, L. E., and King, H. H. C., "Rapid Prediction of High-Alpha Unsteady Aerodynamics of Slender-Wing Aircraft," *Journal of Aircraft*, Vol. 29, No. 2, 1992, pp. 85–92.

[9]Boisseau, P. C., "Investigations of the Low-Subsonic Flight Characteristics of a Model of a Reentry Vehicle with a Thick Flat 75° Swept Delta Wing and a Half-Cone Fuselage," NASA TN D-1007, Feb. 1962.

[10]Ericsson, L. E., and Reding, J. P., "Dynamic Support Interference in High-Alpha Testing," *Journal of Aircraft*, Vol. 23, No. 12, 1986, pp. 889–896.

[11]Ericsson, L. E., "The Fluid Mechanics of Slender Wing Rock," *Journal of Aircraft*, Vol. 21, No. 5, 1984, pp. 322–328.

[12]Ericsson, L. E., "Analytic Prediction of the Maximum Amplitude of Slender Wing Rock," *Journal of Aircraft*, Vol. 26, No. 1, 1989, pp. 35–39.

[13]Nguyen, L. E., Yip, L. P., and Chambers, J. R., "Self-Induced Wing Rock of Slender Delta Wings," AIAA Paper 81-1883, Aug. 1981.

[14]Levin, D., and Katz, J., "Dynamic Load Measurements with Delta Wings Undergoing Self-Induced Roll Oscillations," *Journal of Aircraft*, Vol. 21, No. 1, 1984, pp. 30–36.

[15]Ericsson, L. E., "Slender Wing Rock Revisited," *Journal of Aircraft*, Vol. 30, No. 3, 1993, pp. 352–356.

[16]Ericsson, L. E., and Reding, J. P., "Fluid Mechanics of Dynamic Stall, Part I, Unsteady Flow Concepts," *Journal of Fluids and Structures*, Vol. 2, No. 1, 1988, pp. 1–33.

[17]Lambourne, N. C., Bryer, D. W., and Maybrey, J. F. M., "Pressure Measurements on a Model Delta Wing Undergoing Oscillatory Deformation," Aeronautical Research Council, NPL Aero Rept. 1314, Great Britain, March 1970.

[18]Lambourne, N. C., and Bryer, D. W., "The Bursting of Leading-Edge Vortices—Some Observations and Discussion of the Phenomenon," Aeronautical Research Council, R&M 3282, Great Britain, April 1961.

[19]Ericsson, L. E., and Reding, J. P., "Approximate Nonlinear Slender Wing Aerodynamics," *Journal of Aircraft*, Vol. 14, No. 12, 1977, pp. 1197–1204.

[20]Werlé, H., "Vortices from Very Slender Wings," *La Recherche Aérospatiale*, No. 1009, Nov.–Dec. 1965, pp. 1–12.

[21]Ericsson, L. E., and Reding, J. P., "Unsteady Aerodynamic Analysis of Space Shuttle Vehicles. Part II: Steady and Unsteady Aerodynamics of Sharp-Edged Delta Wings," NASA CR-120123, Aug. 1973.